

Chapter 3

Deposition of Sulfur and Nitrogen



Abington, Connecticut (ABT147)

Sulfur and nitrogen transport and deposition into ecosystems are primarily accomplished through dry and wet atmospheric processes. Modeled dry deposition velocities were combined with measured concentration data to estimate dry deposition fluxes. Wet deposition measurements were obtained from NADP/NTN to estimate wet deposition. The lower deposition rates of total atmospheric sulfur measured during 2001 continued the downward trend that began with the 1995 implementation of the Phase I SO₂ emission reductions. Nitrogen deposition rates also declined from previous levels but were more related to reduced precipitation than to reduced nitrogen air pollution.

This chapter presents information on atmospheric deposition of sulfur and nitrogen. Dry deposition fluxes were estimated from modeled deposition velocities and measured concentration data. Maps of dry deposition fluxes for 2001 are presented. Wet deposition data estimated from NADP/NTN for CASTNet sites for 2001 are also presented. The dry and wet deposition data were combined to estimate total deposition of sulfur and nitrogen. These data were used to estimate the trends in total deposition of sulfur and nitrogen over the 12 years, 1990 through 2001.

Sulfur Deposition

Dry deposition processes were simulated using the MLM described by Meyers *et al.* (1998) and Finkelstein *et al.* (2000). The MLM was run using CASTNet meteorological measurements and information on land use, vegetation, and surface

conditions to calculate deposition velocities for SO₂, HNO₃, O₃, and particles. Deposition velocities were calculated for each hour with valid meteorological data for each CASTNet site for the entire period 1990 through 2001.

The MLM has been evaluated for a limited number of vegetation types, terrain settings, and time periods (summarized by Baumgardner *et al.*, 2002). The model underestimates SO₂ dry deposition, especially for forested settings. The bias of the model for SO₂ deposition simulations is small for crops and grass. Overall, the MLM exhibits a small positive bias for HNO₃. The model has not been evaluated rigorously for particles. Vegetation data from eleven sites were added to the CASTNet database for these simulations.

The eleven sites include:

- Acadia National Park, ME (ACA416),
- Great Smoky Mountains National Park, TN (GRS420),
- Everglades National Park, FL (EVE419),
- Virgin Islands National Park (VII423),
- Theodore Roosevelt National Park, ND (THR422),
- Olympic National Park, WA (OLY421),
- Denali National Park, AK (DEN417),
- Yukon Flats National Wildlife Refuge, AK – Poker Flats (POF425),
- Hawaii Volcanoes National Park, HI (HVT424),
- Hoxeyville, MI (HOX148), and
- Indian River Lagoon, FL (IRL141).

The model and aggregation procedures were summarized in Chapter 1 of the CASTNet 2000 Annual Report (Harding ESE, 2002a).

MLM simulations were done separately for SO_2 and SO_4^{2-} . The model calculations were summed to obtain estimates of dry sulfur deposition (as S), which are shown in Figure 3-1 for 2001. The map shows a narrow region along and downwind of the Ohio River Valley from southern Indiana and northern Kentucky to New Jersey with fluxes greater than 5.00 kilograms per hectare per year (kg/ha/yr). The highest deposition rates were estimated for VIN140 and Pennsylvania State University (PSU106) with fluxes of 7.33 and 7.39 kg/ha/yr , respectively. The flux data show sharp downward gradients from the Ohio Valley northward into New England and also into Wisconsin and Minnesota. The dry deposition rates for the western sites were all less than 1.00 kg/ha/yr and generally less than 0.50 kg/ha/yr . The MLM was not run for those sites in Figure 3-1 having no

numerical value adjacent to the site location because of incomplete data.

Figure 3-2 depicts the percentage of dry sulfur deposition that resulted from deposition of SO_2 . The map shows that SO_2 was the major contributor to dry deposition. The percentage was generally above 80 percent for most of the eastern sites and approximately 90 percent for those sites near major source regions. The percentages were lower for a large majority of the western sites because of their remote locations, distances from major sources, and the relatively lower V_d simulated for these more arid sites (Appendix C). Figures 3-3 and 3-4 provide maps of 2001 dry deposition fluxes of SO_2 and SO_4^{2-} as S, respectively.

Wet deposition values represent a combination of historical CASTNet wet deposition data with NADP/NTN wet deposition data. For CASTNet sites where wet concentrations were measured prior to January 1999 (when responsibility for wet deposition monitoring activities at CASTNet sites was transferred to NADP/NTN), those values were used in the data set. For sites where no wet concentrations were measured and for all sites after January 1999, values were obtained from a grid of concentration estimates derived from available NADP/NTN sites by using an inverse distance weighting function. Estimated concentrations were multiplied by the precipitation measured at the CASTNet sites to obtain estimates of wet deposition.

Figure 3-5 presents wet deposition fluxes of SO_4^{2-} (as S) for 2001. The map shows a large area of wet deposition in excess of 5.00 kg/ha/yr from eastern Tennessee to southern New York. Ohio recorded the highest rates of wet deposition. In general, the extent and magnitude of the high wet sulfur fluxes were smaller than those for 2000. Values at western sites were generally less than 1.00 kg/ha/yr , except

for the three reporting sites in Washington and Chiricahua National Monument, AZ (CHA467).

Information on mean volume-weighted concentrations of sulfate in precipitation and mean precipitation amounts for the 34 eastern reference sites is shown in Figure 3-6 for the 12 years, 1990 through 2001. The figure shows the significant decrease in SO_4^{2-} concentrations in 1995, the gradual rise through 1998, and the decline over the last three years. The figure also illustrates the

significant variability in precipitation. The year 2001 recorded the lowest mean precipitation amount over the 12-year period. Figure 3-7 summarizes wet and dry sulfur deposition over the 12-year period. Both wet and dry deposition rates decreased significantly. Wet deposition showed more interannual variability and followed the trend in precipitation fairly closely. Dry deposition contributed approximately 40 percent of total deposition.

Trends in Dry Deposition at Fifteen Western Sites

Concentrations of sulfur and nitrogen species, meteorological measurements, and supporting vegetation data were available for 15 western sites over the period 1995 through 2001. The data were used to simulate dry deposition of sulfur and nitrogen. The MLM simulations of mean annual fluxes for the 15 sites were aggregated to provide estimates in trends over the seven years. The aggregated fluxes show a downward trend in dry nitrogen deposition and no trend in dry sulfur deposition.

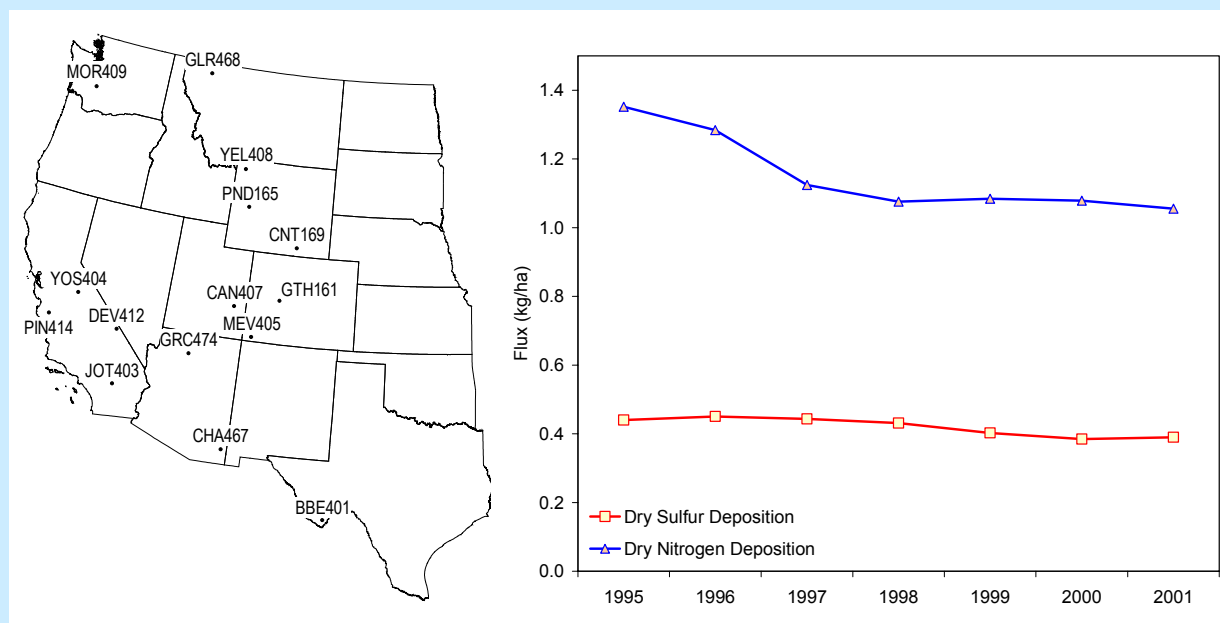


Figure 3-8 provides a map of estimates of total sulfur deposition. The map was constructed by adding dry and wet deposition (i.e., the values in Figures 3-1 and 3-5). The circles in the figure illustrate the magnitude of total sulfur deposition and also the relative contributions from wet and dry deposition. The green shading signifies wet deposition and the blue shows dry deposition. The map shows a narrow region with sulfur deposition above 10.00 kg/ha/yr. The region extends from southwestern Indiana along the Ohio River into Pennsylvania, Maryland, and New Jersey. Sharp downward gradients (factor of 3.0) were observed from New York to Maine and Illinois to Minnesota. Sulfur deposition at western sites was generally less than 2.00 kg/ha/yr, except for OLY421, which had a value of 3.26.

The maps in Figures 3-3 through 3-5 illustrate the relative contributions of dry SO_2 , dry SO_4^{2-} , and wet SO_4^{2-} to total sulfur deposition. Comparison of the deposition rates showed that wet sulfur deposition was the major contributor to total sulfur deposition (Figure 3-8), followed by dry SO_2 , and a much smaller contribution from dry SO_4^{2-} .

Figure 3-9 presents a box plot that shows the trend in annual total (dry + wet) sulfur deposition (as S) over the 12 years, 1990 through 2001. The box plot was based on data obtained from the 34 eastern reference sites. Total sulfur deposition declined significantly over the 12 years.

Nitrogen Deposition

Figure 3-10 presents a map of dry fluxes of nitrogen ($\text{HNO}_3 + \text{NO}_3^- + \text{NH}_4^+$, as N) for 2001. This map was constructed by summing the individual MLM simulations for the three species. Approximately half of the CASTNet sites in the eastern United States observed dry nitrogen deposition above 2.00 kg/ha/yr, although the geographic pattern is

complex. Two areas showed fluxes above 3.00 kg/ha/yr – Ohio to northern Kentucky and southeastern Pennsylvania to northern Virginia. Outside of these areas, a single value of 3.75 kg/ha/yr was observed in Tennessee at GRS420. The values at the western sites ranged from 0.22 kg/ha/yr in Glacier National Park, MT (GLR468) to 2.76 kg/ha/yr at JOT403. The MLM simulated a region in southern California with fluxes in excess of 2.00 kg/ha/yr.

Figures 3-11 through 3-13 illustrate the dry nitrogen deposition (as N) that was produced by HNO_3 , NO_3^- , and NH_4^+ , respectively. The figures show that dry HNO_3 deposition was the principal contributor to dry nitrogen deposition.

A map of 2001 wet deposition of NO_3^- plus NH_4^+ (as N) is given in Figure 3-14. The figure shows a large area from the Midwest (Wisconsin to Kentucky) eastward to New Jersey with deposition rates in excess of 5.00 kg/ha/yr. Values at the western sites ranged from 0.53 kg/ha/yr at LAV410 to 2.17 kg/ha/yr at Centennial, WY (CNT169).

Mean volume-weighted concentrations of nitrate and NH_4^+ in precipitation and mean precipitation amounts are shown in Figure 3-15. The figure shows no significant change in NO_3^- and NH_4^+ concentrations over the 12 years. On the other hand, precipitation amounts over the last three years were well below the 12-year average. Figure 3-16 provides the trends in wet and dry nitrogen deposition. The figure shows no change in dry deposition but suggests a decline in wet deposition. This trend is related more to precipitation amounts than to changes in nitrogen pollution. Dry deposition of nitrogen represented about a third of total deposition.

A map (Figure 3-17) of total nitrogen deposition (as N) for 2001 was constructed by summing the

estimates of dry (blue) and wet (green) deposition. The figure shows that the majority (all but nine) of the eastern sites recorded deposition rates above 5.00 kg/ha/yr. Values above 10.00 kg/ha/yr were observed in Ohio. Lower fluxes were recorded along the peripheries of the network (e.g., in New England and Florida and throughout the west). The values at the western sites ranged from 1.16 kg/ha/yr at OLY421 to 4.62 kg/ha/yr at JOT403.

The maps in Figures 3-11 through 3-14 illustrate the relative contributions of dry and wet nitrogen

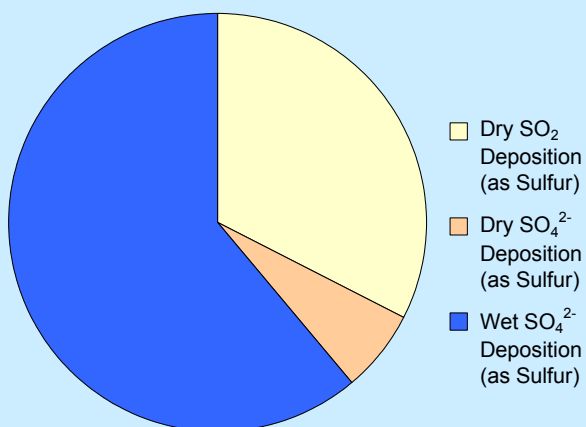
species to total deposition. Comparison of the deposition rates in Figures 3-11 through 3-13 to those in Figure 3-14 showed that wet nitrogen ($\text{NO}_3^- + \text{NH}_4^+$) deposition was the largest contributor to total nitrogen deposition (Figure 3-17), followed by dry HNO_3 , dry NH_4^+ , and dry NO_3^- .

Figure 3-18 presents a box plot that shows the trend in total nitrogen deposition over the 12 years, 1990 through 2001. This decline is more related to reduced precipitation than to reduced nitrogen in the atmosphere.

Contributors to 2001 Atmospheric Deposition

CASTNet data show that wet sulfate deposition was the major contributor to total sulfur deposition, followed by dry SO_2 and a much smaller contribution from dry SO_4^{2-} . Dry deposition contributed about 40 percent of total sulfur deposition. Wet NO_3^- deposition was the major contributor to total nitrogen deposition followed by wet NH_4^+ , dry HNO_3 , dry NH_4^+ , and dry NO_3^- . Dry deposition contributed approximately one third of total nitrogen deposition.

Sulfur



Nitrogen

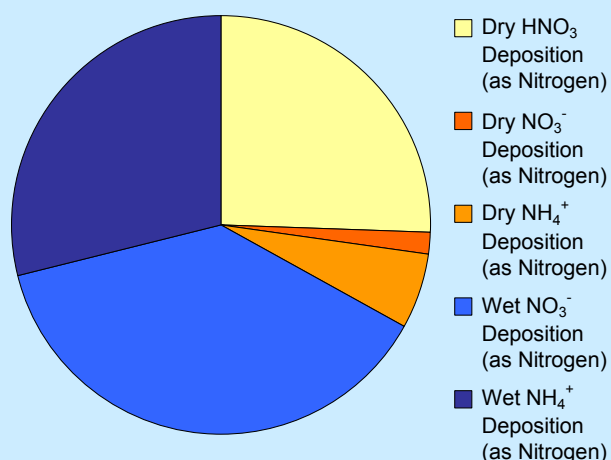
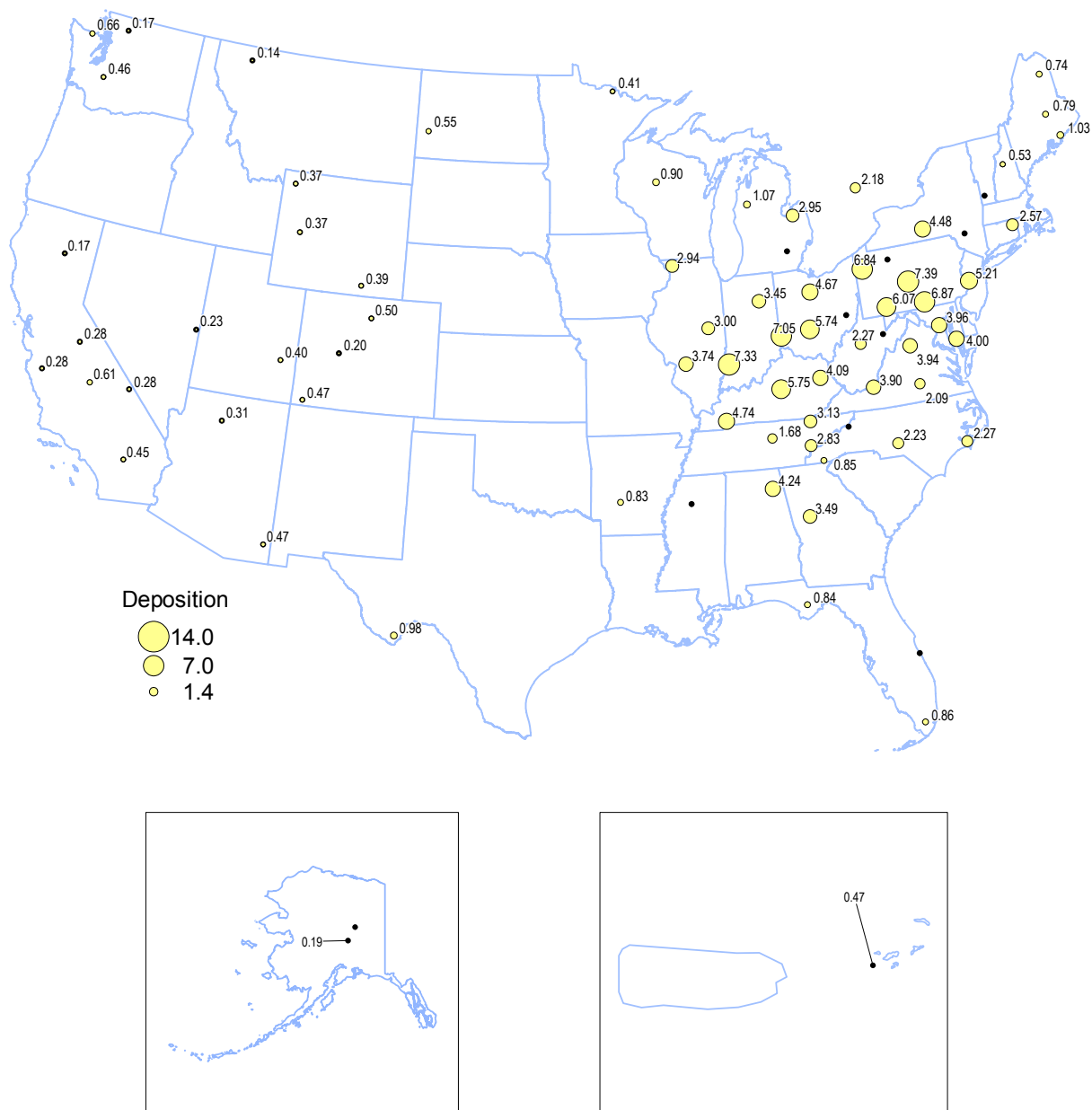


Figure 3-1. Total Dry Sulfur ($\text{SO}_2 + \text{SO}_4^{2-}$) Deposition (as S) (kg/ha/yr) for 2001



Note: Hawaii is not included with the Chapter 3 maps because there are no valid deposition values for 2001.

Figure 3-2. Percentage of Total Dry Sulfur Deposition from SO₂ for 2001

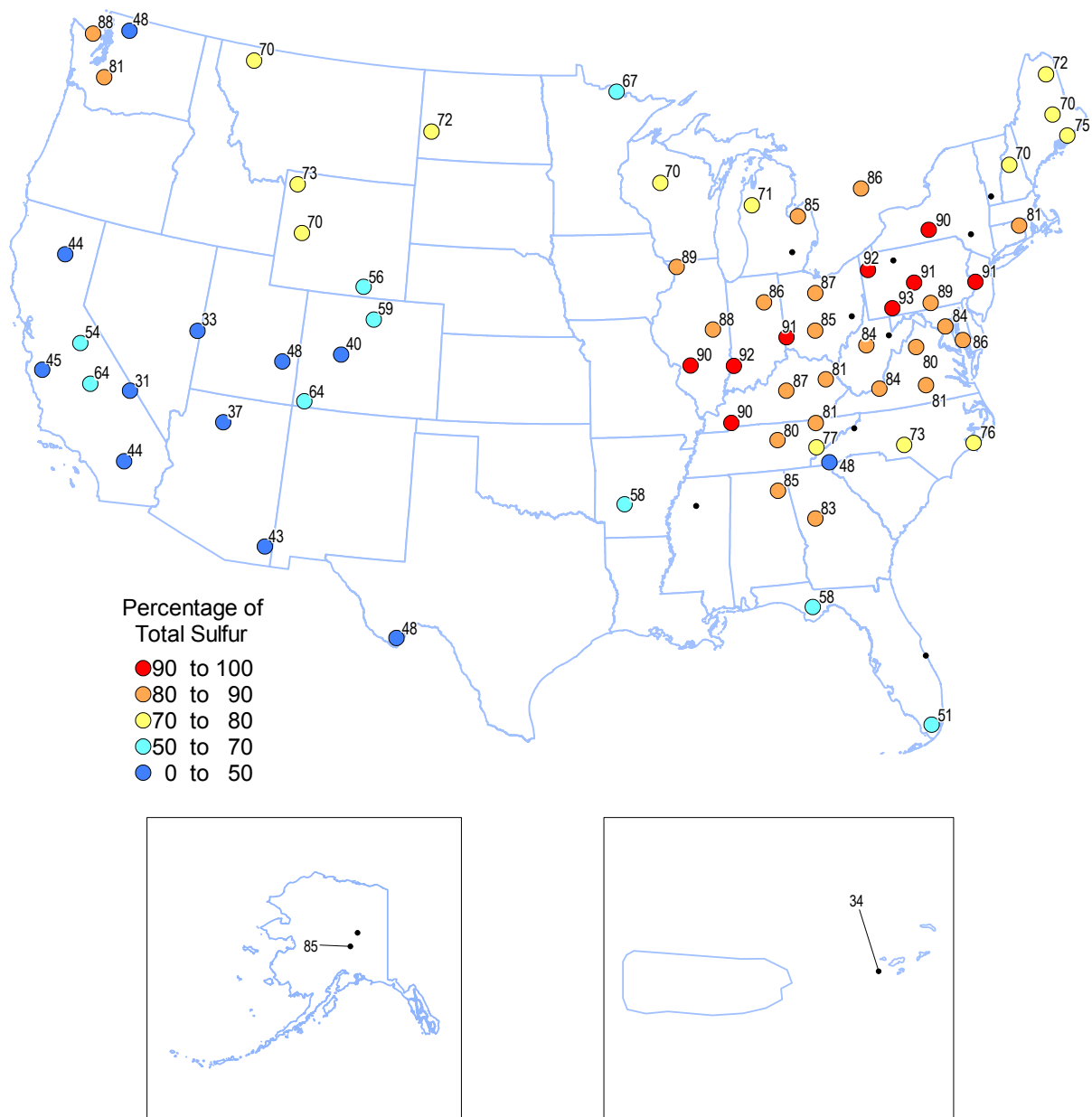


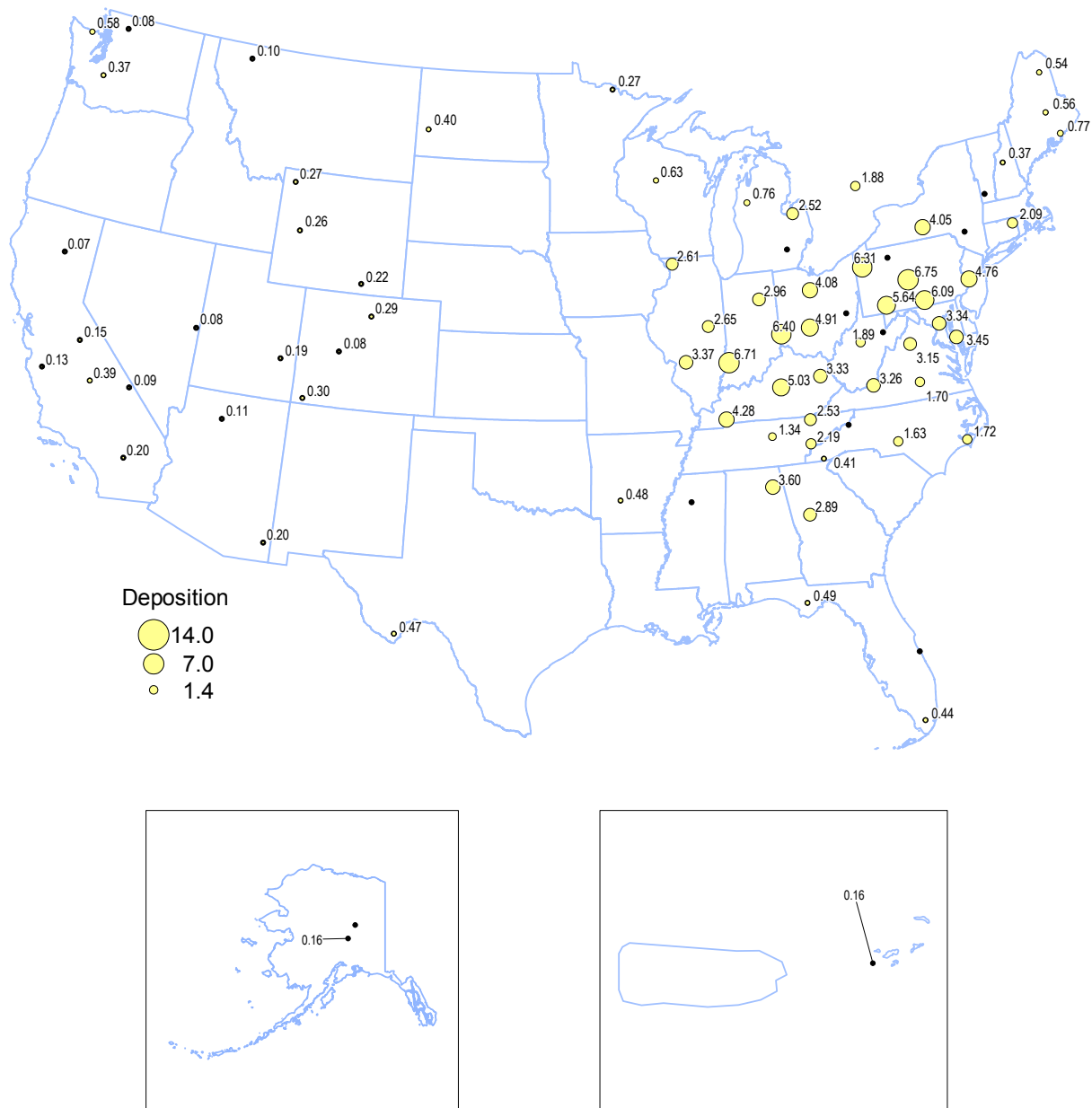
Figure 3-3. Dry SO₂ Deposition (as S) (kg/ha/yr) for 2001

Figure 3-4. Dry SO_4^{2-} Deposition (as S) (kg/ha/yr) for 2001



Figure 3-5. Wet SO_4^{2-} Deposition (as S) (kg/ha/yr) for 2001

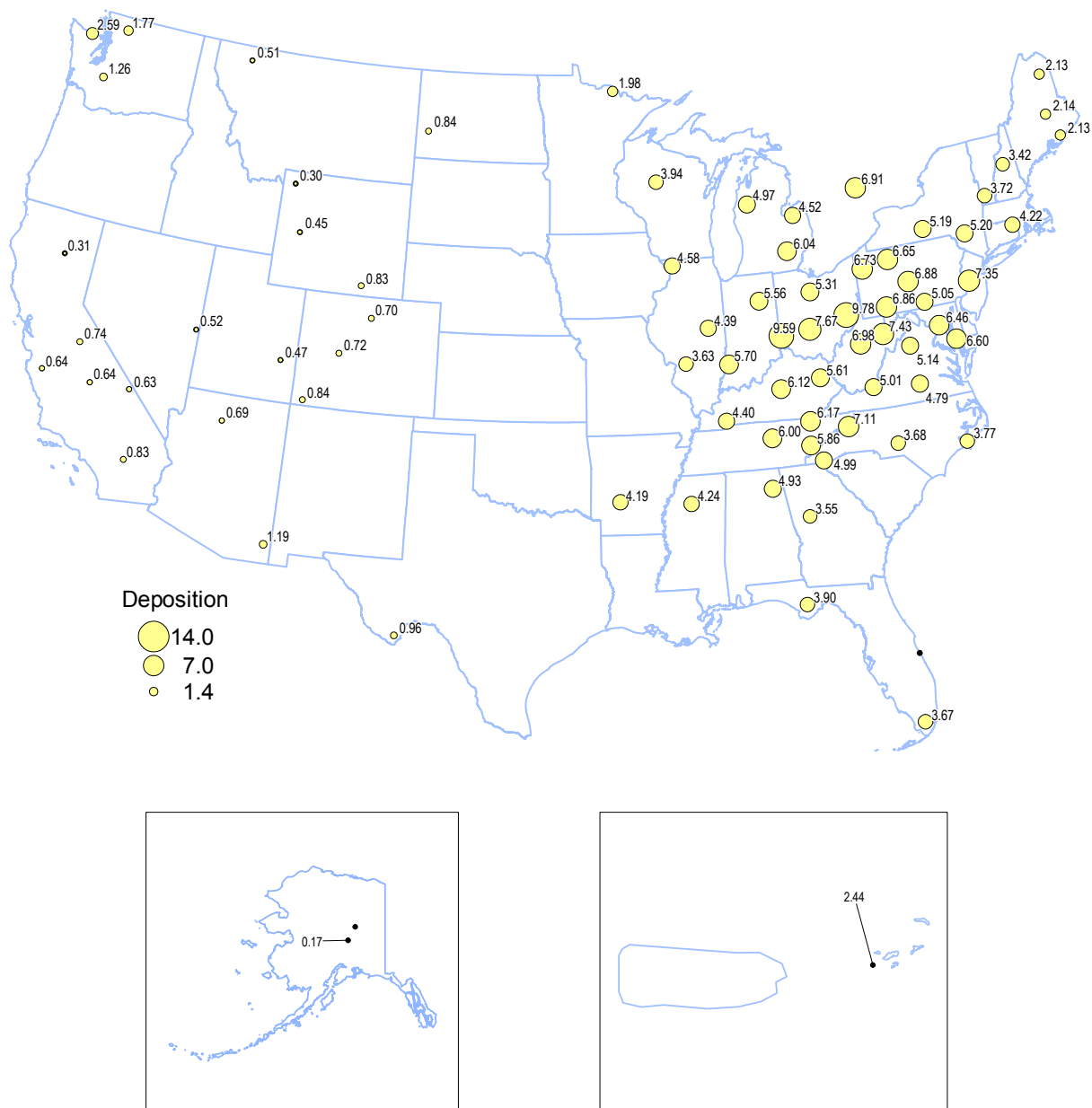


Figure 3-6. Trend in SO_4^{2-} Concentrations in Precipitation and Annual Total Precipitation – Eastern Reference Sites

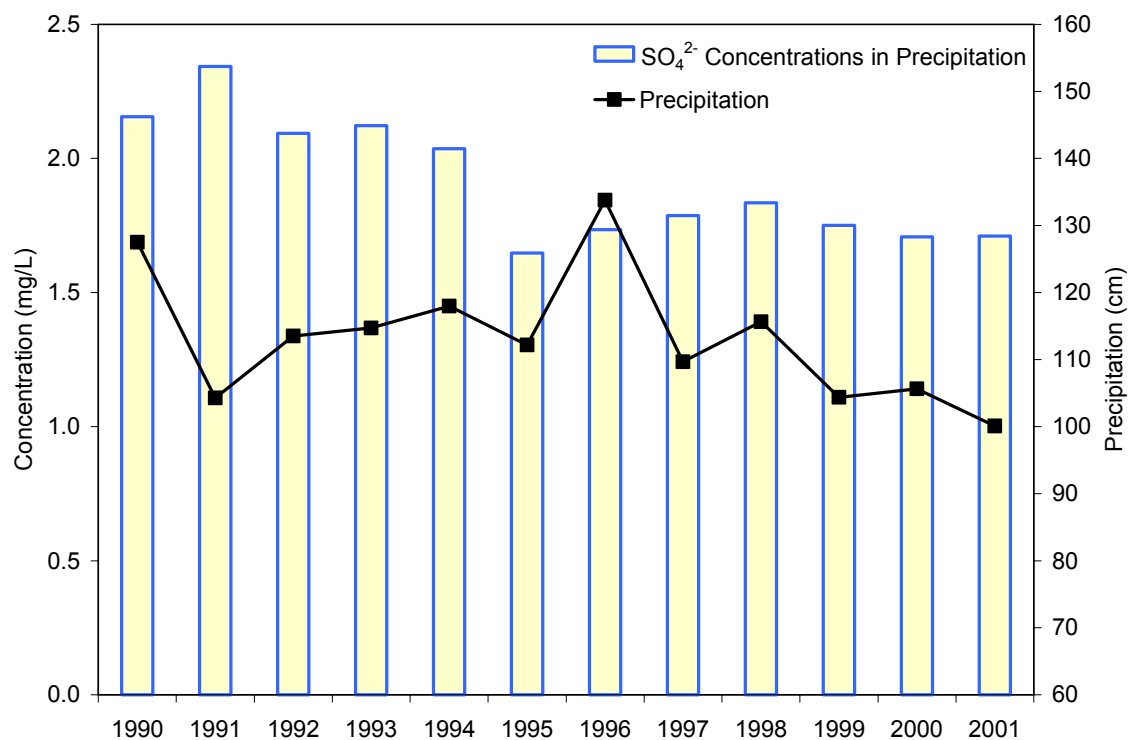


Figure 3-7. Trend in Total Dry and Total Wet Sulfur Deposition – Eastern Reference Sites

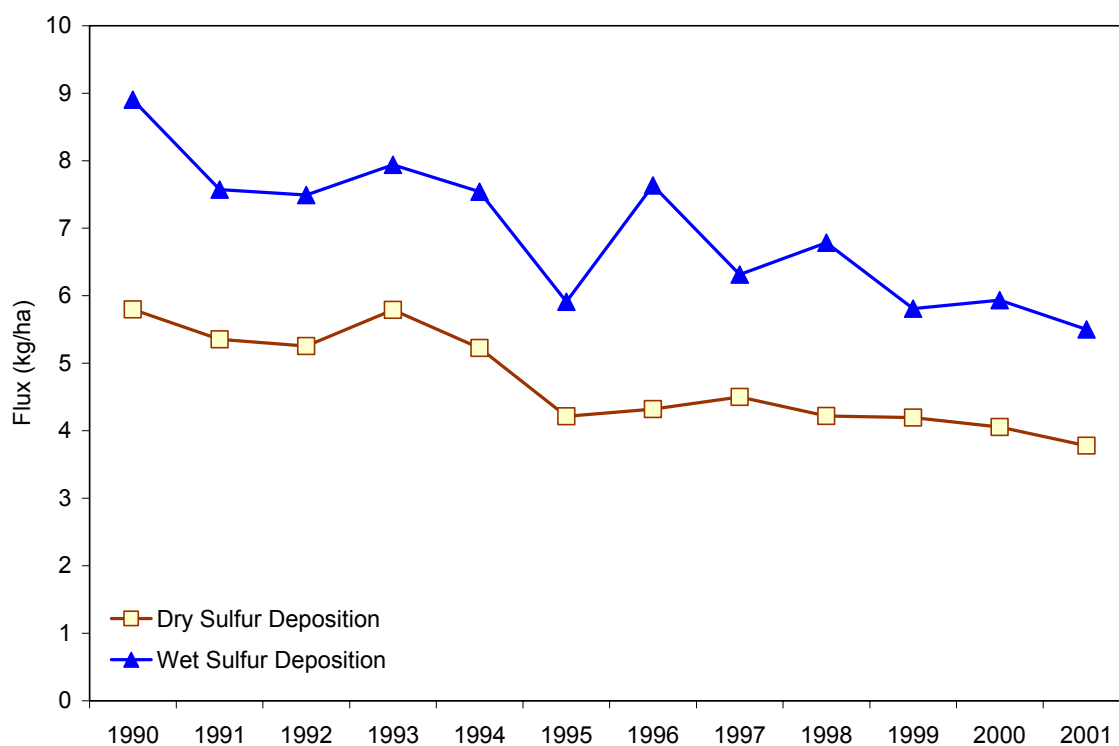


Figure 3-8. Total (Dry + Wet) SO_4^{2-} Deposition (as S) (kg/ha/yr) for 2001

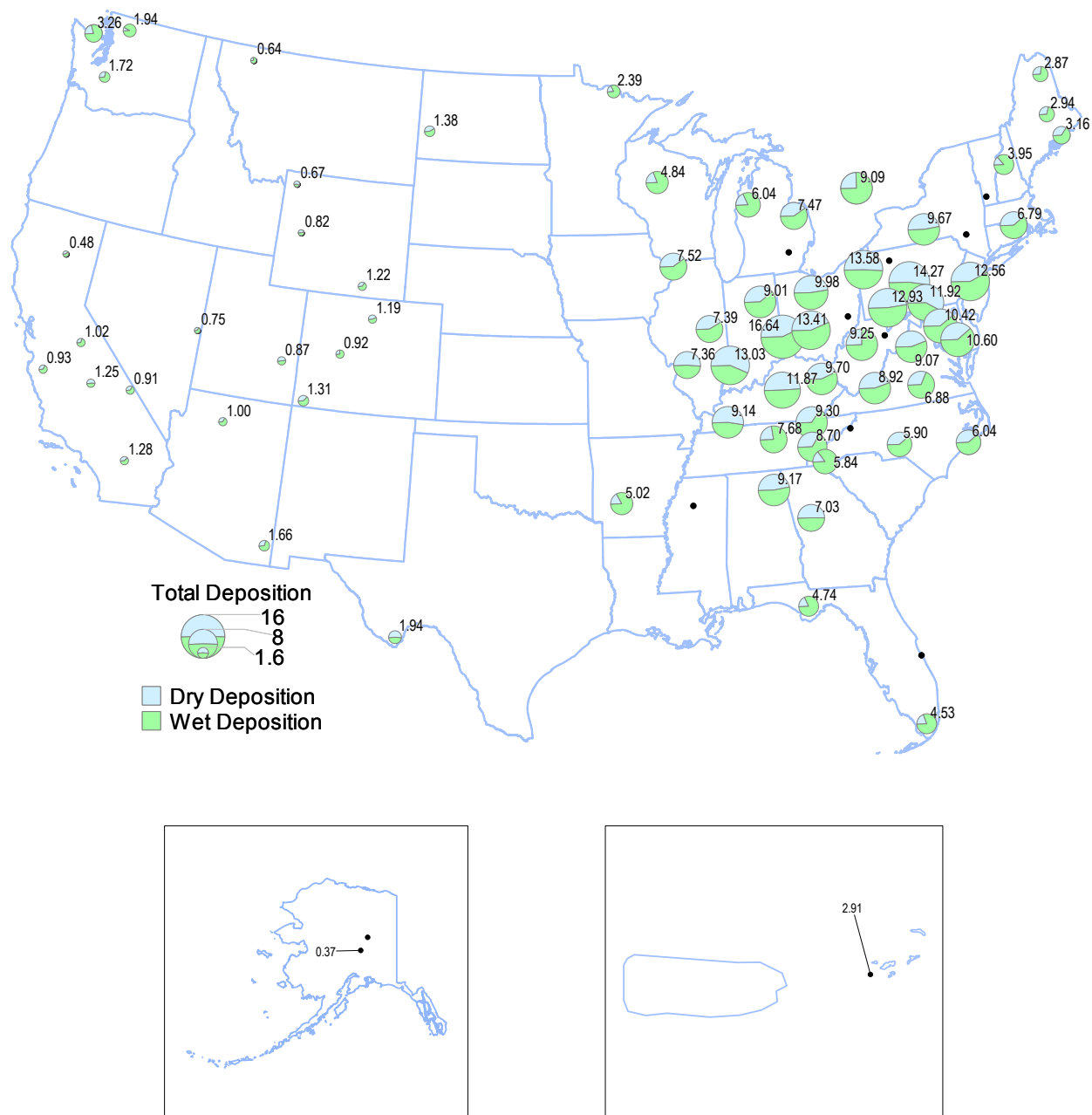


Figure 3-9. Trend in Annual Total (Dry + Wet) Sulfur Deposition (as S) (kg/ha/yr) – Eastern United States

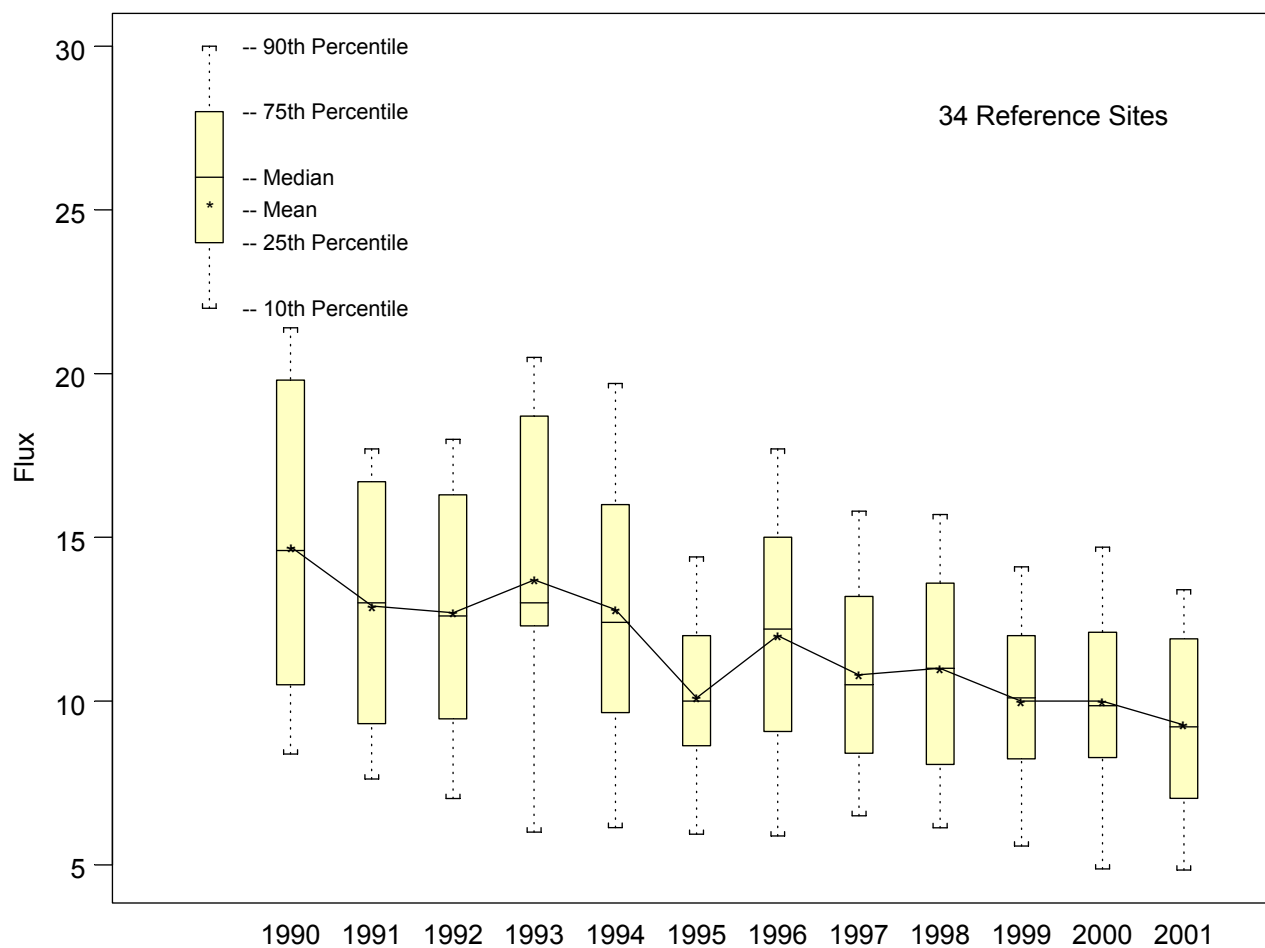


Figure 3-10. Total Dry Nitrogen ($\text{HNO}_3 + \text{NO}_3^- + \text{NH}_4^+$) Deposition (as N) (kg/ha/yr) for 2001

Figure 3-11. Dry HNO_3 Deposition (as N) (kg/ha/yr) for 2001



Figure 3-12. Dry NO_3^- Deposition (as N) (kg/ha/yr) for 2001

Figure 3-13. Dry NH_4^+ Deposition (as N) (kg/ha/yr) for 2001

Figure 3-14. Wet Nitrogen ($\text{NO}_3^- + \text{NH}_4^+$) Deposition (as N) (kg/ha/yr) for 2001

Figure 3-15. Trend in NO_3^- and NH_4^+ Concentrations in Precipitation and Annual Total Precipitation – Eastern Reference Sites

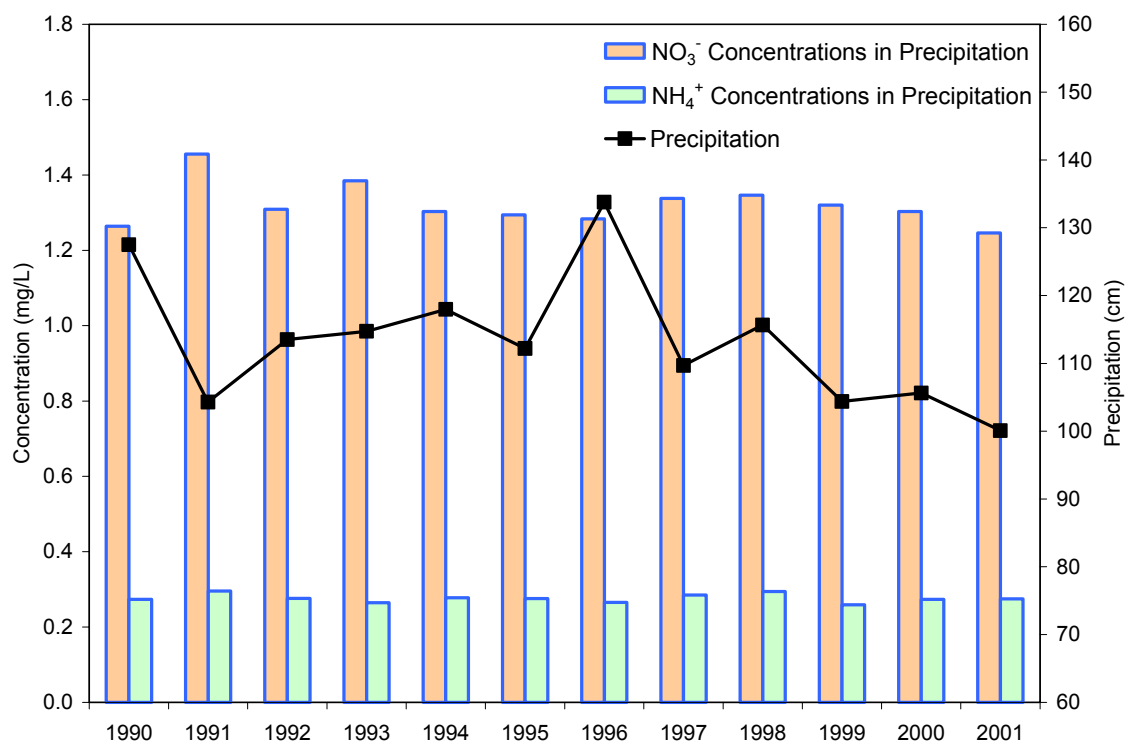


Figure 3-16. Trend in Total Dry and Total Wet Nitrogen Deposition – Eastern Reference Sites

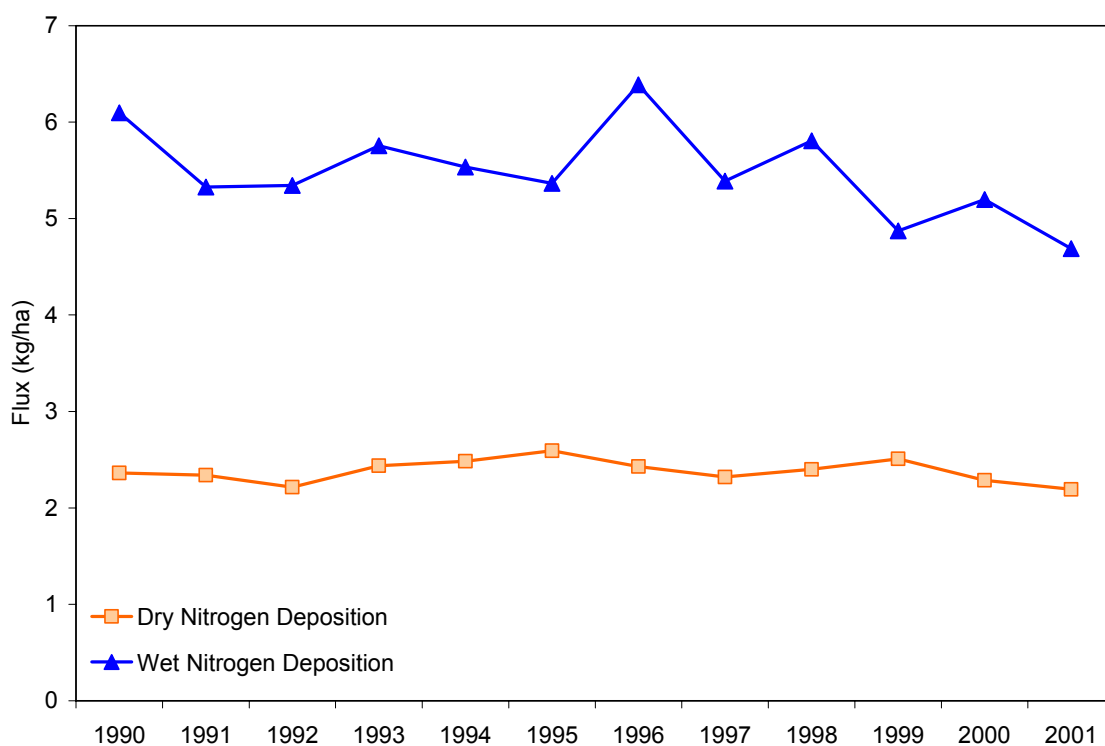


Figure 3-17. Total (Dry + Wet) Nitrogen Deposition (as N) (kg/ha/yr) for 2001

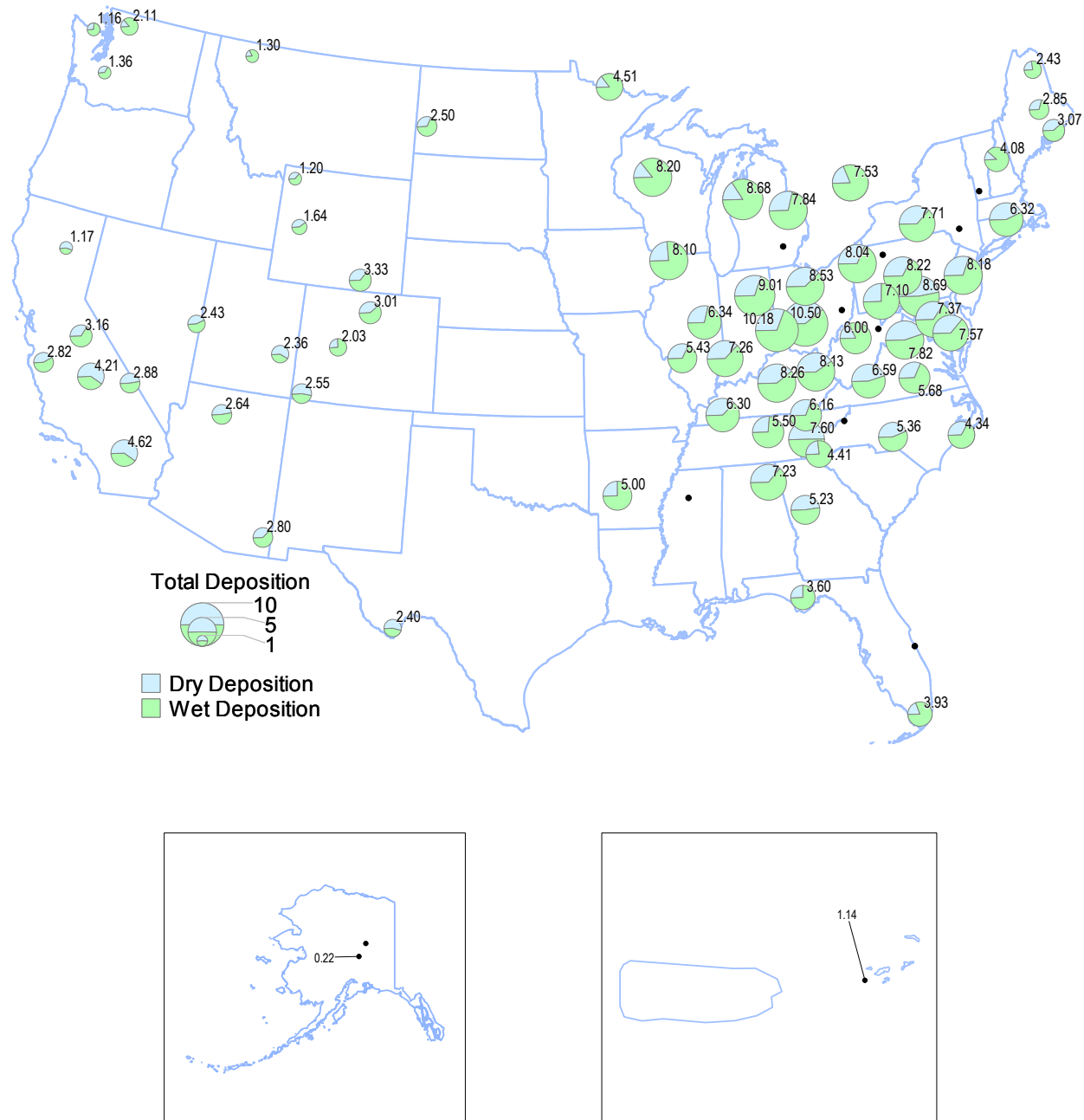
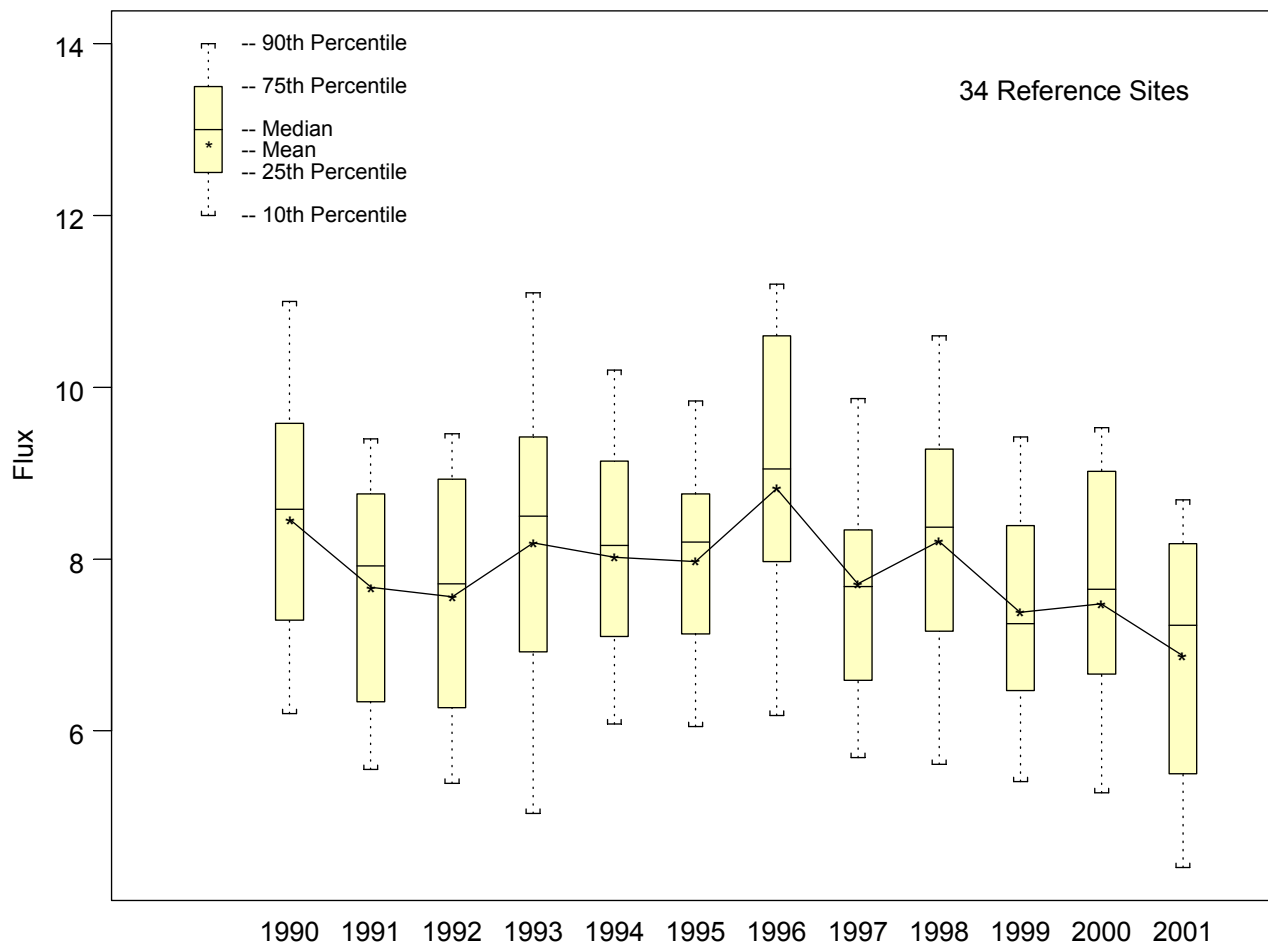


Figure 3-18. Trend in Annual Total (Dry + Wet) Nitrogen Deposition (as N) (kg/ha/yr) – Eastern United States



This page intentionally left blank.